

Morphology and Luminescence Properties of ZnO layers produced by Magnetron Sputtering

Emil RUSU¹, Irina GHIŢU¹, Vladimir PRILEPOV², Victor ZALAMAI³, Veaceslav URSAKI³

¹*Institute of Electronic Engineering and Nanotechnologies, Academy of Sciences of Moldova, Academy str. 3/3, Chisinau MD-2028, Republic of Moldova, e-mail: rusue@lises.asm.md*

²*State University of Moldova, Mateevici str. 60, Chisinau MD-2009, Moldova*

³*Institute of Applied Physics of the Academy of Sciences of Moldova, Academy str. 5, Chisinau MD-2028, Moldova*

Abstract – We show that the morphology and the luminescence properties of ZnO layers produced by magnetron sputtering can be controlled by technological parameters of sputtering, particularly by the ratio of argon to oxygen gases in the gas flow during the growth process. Smooth and flat layers were produced with a high Ar/O ratio, while porous layers with various morphologies were obtained with a low Ar/O ratio. The layers produced with O/Ar ration equal to 10 exhibit extremely high near-bandgap luminescence intensity even higher in comparison with bulk ZnO single crystals. The free carrier density estimated from the analysis of photoluminescence spectra is also very high in these samples suggesting that these technological conditions promote both optical and electrical activation of the doping Al impurity. The samples grown with high Ar/O ratios exhibit strong visible emission which is controlled by the technological conditions.

Index Terms – ZnO, magnetron sputtering, morphology, luminescence, excitonic emission, deep centers.

I. INTRODUCTION

ZnO demonstrates increasing fundamental interest and technological applications due to its wide and direct band gap (3.37 eV at room temperature), large exciton binding energy (60 meV), large bond strength (with a cohesive energy of 1.89 eV), and large mechanical stability (with a melting point of about 2200 K) [1], it being of a particular interest for optoelectronic and photonic devices [2-4].

In recent years, with the development of different growth techniques, gallium nitride (GaN) has become the most important building block for LEDs operating in the green to ultraviolet light range [5-7]. ZnO and GaN are analogous materials with many similar properties. ZnO has an advantage over GaN, due to the availability of high quality ZnO substrates, while there is a lack of GaN substrates. This makes possible the preparation of ZnO based homojunction in addition to heterojunctions.

A multitude of synthesis methods, such as various wet chemical methods [8-12], sol-gel methods [13,14], metal organic chemical vapour deposition (MOCVD) [15-17], molecular beam epitaxy (MBE) [18,19], electrochemical deposition [20-22], metal-catalyzed vapour-liquid-solid (VLS) growth [3,23], and thermal chemical vapour transport and condensation method without metal catalysts [24-28] have been employed for the fabrication of ZnO layers.

Such methods as chemical, electrochemical, sol-gel, VLS, and chemical vapour transport and condensation growth are cost effective. However, they basically lead to the production of nanostructured layers, such as wires, rods, ribbons, belts, tubes, discs, tetrapods, combs, rings, springs, propeller arrays, etc, it being hard to produce smooth and flat layers with these techniques. Smooth and flat films are highly desired in homojunction and heterojunctions. Smooth surfaces can be obtained with MOCVD and MBE methods. However, these technologies are quite expensive. Magnetron

sputtering is a technique which allows one to produce both nanostructured and flat layers, in being at the same time less expensive than MOCVD and MBE technologies.

In this work, we investigate the morphology and the photoluminescence (PL) properties of ZnO layers produced by magnetron sputtering in order to establish their dependence upon the technological conditions of growth.

II. SAMPLE PREPARATION AND EXPERIMENTAL DETAILS

Magnetron sputtering of ZnO films was performed in an installation assembled on the basis of a VUP-5 instrument. A control sample was placed in the sputtering chamber near the Si, SiO₂/Si, or ITO-on-glass basic support for monitoring the deposition process via measuring the resistivity of the layer deposited on the control sample. A 99,99 % purity Zn plate with a diameter of 40 mm and thickness of 5 mm doped with 2% wt of Al was used as target. The temperature of both the control and the basic supports was maintained at a temperature from the interval 200 – 220 °C, while the magnetron power was $W=360 \text{ V} \times 100 \text{ mA}$. The Si support was treated in a 30% Na₂S₂O₃x5H₂O solution before the sputtering process for improving the adhesion of the deposited ZnO layer.

A mixture of Ar+O was used as working gas. The ratio of Ar/O in the gas flow was changed and air was introduced in the growth chamber for a certain period of time during the sputtering process in order to controll morphology and the raditive properties of the deposited ZnO film. The samples were annealed in air during 30 min at 450 °C after the deposition process.

A VEGA TESCAN TS 5130 MM scanning electron microscope (SEM) was used for morphological characterization of the samples.

Photoluminescence was excited by 325 nm line of a He-Cd Melles Griot laser and was analyzed through a double

spectrometer at low temperature (10 K). The resolution was better than 0.5 meV. The samples were mounted on the cold station of a LTS-22-C-330 cryostat.

emissions can be observed with a peak position varying in a wide wavelength range from 450 to 830 nm.

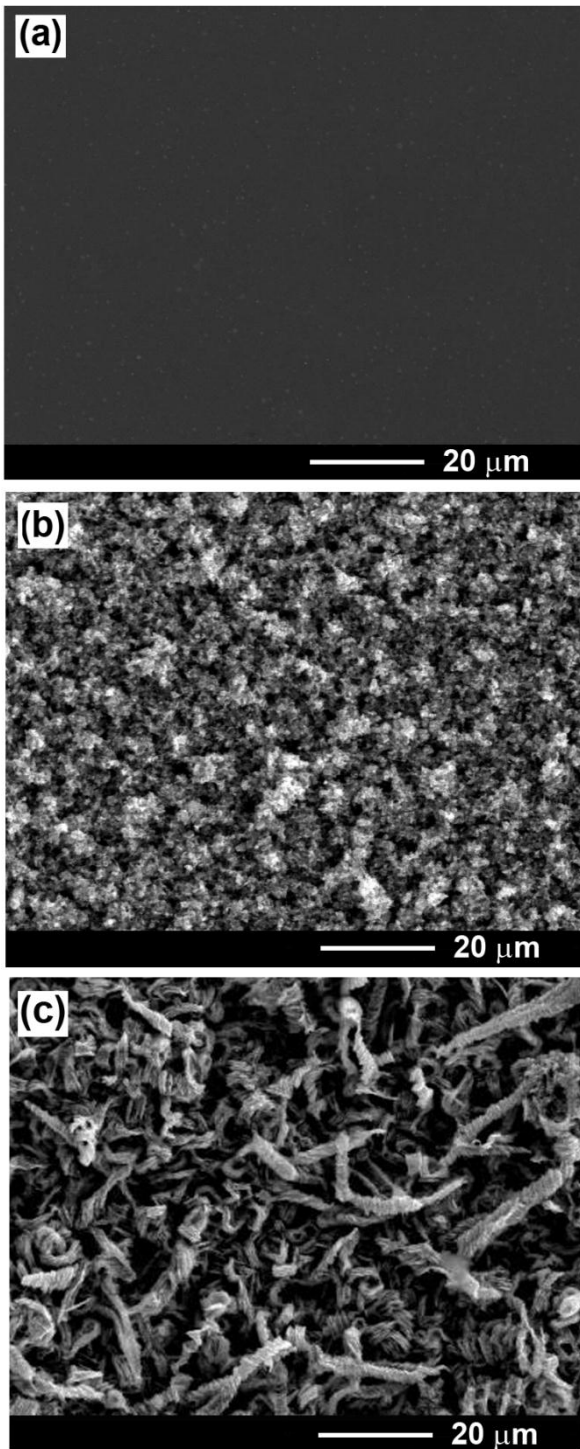


Fig. 1. SEM image of ZnO layers produced by magnetron sputtering in processes with different ratio of argon to oxygen gases in the gas flow during the growth process as follows: Ar:O = 10:1 (a); Ar:O = 1:1 (b); Ar:O = 1:10 (c).

III. RESULTS AND DISCUSSIONS

Wide-gap oxide semiconductors are attractive materials as phosphors if they exhibit visible emissions arising from defect levels in the bandgap. Apart from the near-band-edge ultraviolet emission at approximately 380 nm, ZnO is also known to exhibit a complex luminescence behavior in the visible wavelength region [29,30]. Visible deep-level

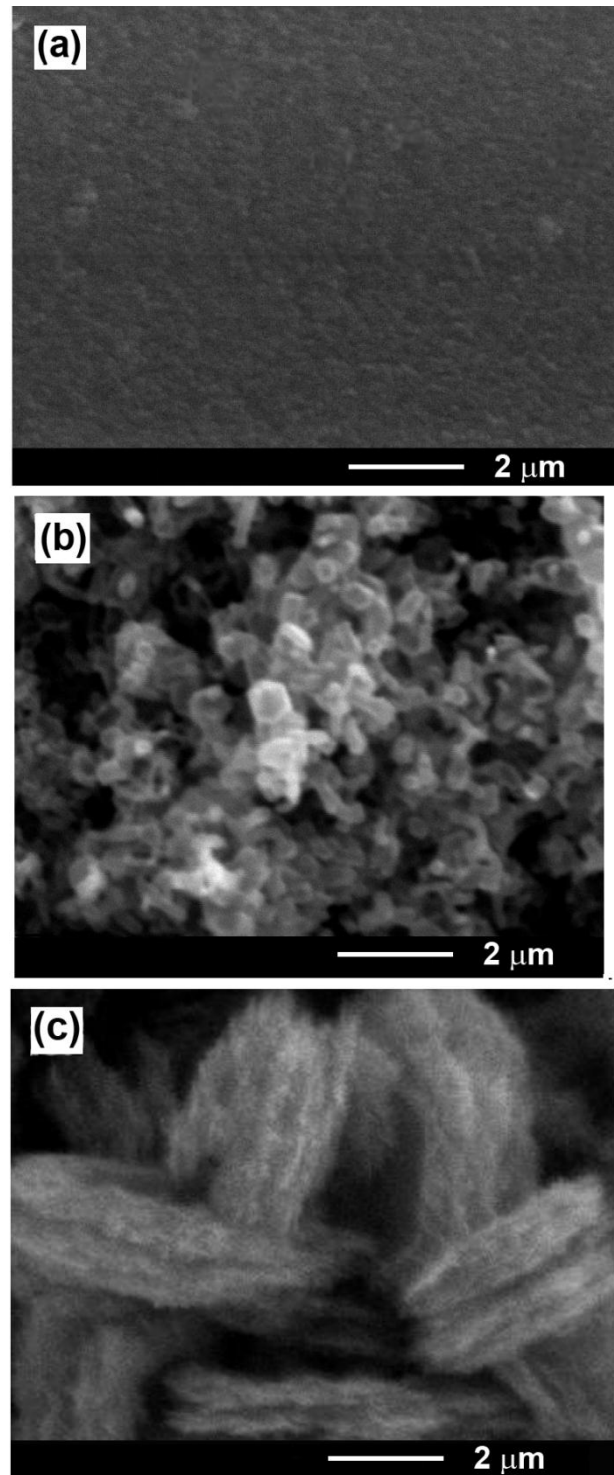


Fig. 2. Enlarged SEM view of ZnO layers produced by magnetron sputtering in processes with different ratio of argon to oxygen gases in the gas flow during the growth process as follows: Ar:O = 10:1 (a); Ar:O = 1:1 (b); Ar:O = 1:10 (c).

Since the defect-related emissions are known to be sensitive to technological conditions of sample preparation, one can expect that the luminescence spectrum from ZnO samples in the visible range as well as the morphology of layers can be controlled by the technological parameters of magnetron sputtering.

The investigation of the morphology as well as the radiative properties of ZnO layers grown by magnetron

sputtering demonstrated that they are determined by the technological conditions such as the pressure of gases in the growth chamber, the concentration of oxygen, as well as by the substrate used. It was found that the introduction of air in the growth chamber for a period of time longer than 30 min during the sputtering process leads to the oxidation of the target. This oxidation, in turn, affects the magnetron power and creates instabilities in plasma maintaining. The velocity of gas flows into the chamber is set to a value assuring the maintenance of a constant pressure, and therefore a stability of the created plasma.

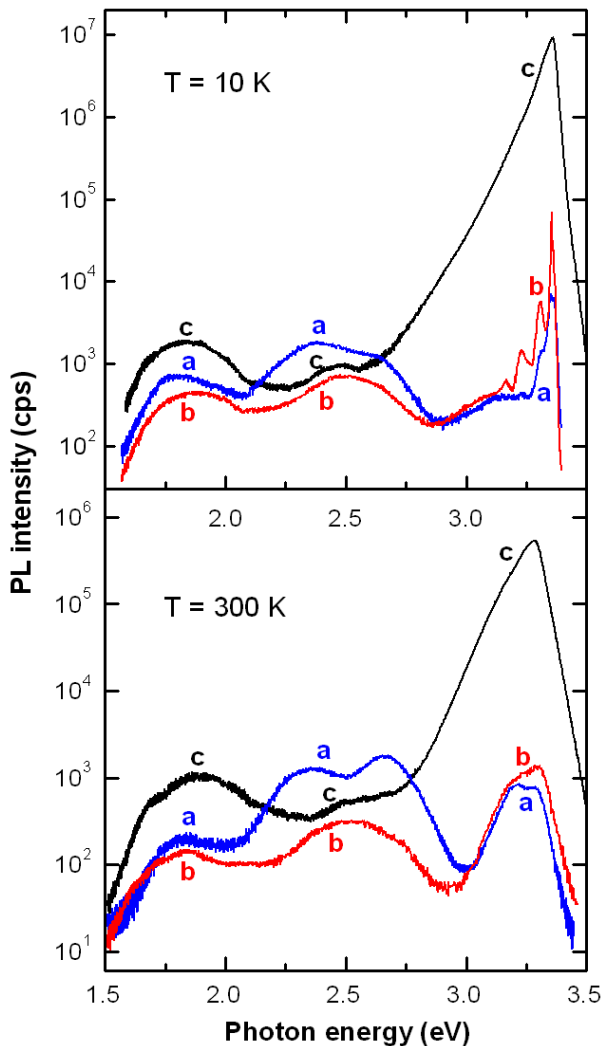


Fig. 3. PL spectra of ZnO layers produced by magnetron sputtering in processes with different ratio of argon to oxygen gases in the gas flow during the growth process as follows: Ar:O = 10:1 (a); Ar:O = 1:1 (b); Ar:O = 1:10 (c). The samples were annealed in air during 30 min at 450 °C after the deposition process

The morphology of the produced ZnO layers was found to be determined first of all by the ratio of argon to oxygen gases in the gas flow during the growth process. High values of the Ar/O ratio result in the production of smooth and flat ZnO films with the morphology illustrated in Fig. 1a for a film produced with the Ar/O ratio equal to 10. The increase of the oxygen content into the gas flow leads to the production of porous layers as shown in Fig. 1b and 1c. When the Ar:O ratio is 1:1, the obtained ZnO layer consists of microcrystallites as shown in Fig. 1b. The size of these crystallites determined from the enlarged view presented in Fig. 2b is around 200 – 500 nm. Further increase of the

oxygen content leads to the creation of spectacularly twisted microstructures (Fig. 1c) which prove to be porous at a more accurate analysis (Fig. 2c). The length of the microstructures produced with an Ar:O ratio of 1:10 on an ITO-on-glass substrate vary in the range of 4 to 20 μm with a diameter of 1 – 4 μm .

Apart from morphology, the ratio of argon to oxygen gases in the gas flow during the growth process strongly influences the radiative properties of the produced ZnO layers. The smooth films produced with a high Ar/O ratio exhibit weak luminescence suggesting an amorphous nature of the film. Annealing of samples in air during 30 min at 450 °C after the deposition process leads to increasing luminescence intensity due to the crystallization [curve (a) in Fig. 3].

Several visible PL bands are observed in the luminescence spectrum in addition to the near band-edge emission. The visible emission from the sample produced with the Ar/O ratio equal to 10 (Fig. 3) consists of three bands located around 1.85 eV, 2.37 eV, and 2.67 eV at both 10 K and room temperature. The near-band-edge luminescence at 10 K is dominated by two bands at 3.61 and 3.71 eV related to the recombination of donor bound excitons (D^0X) (Fig. 4).

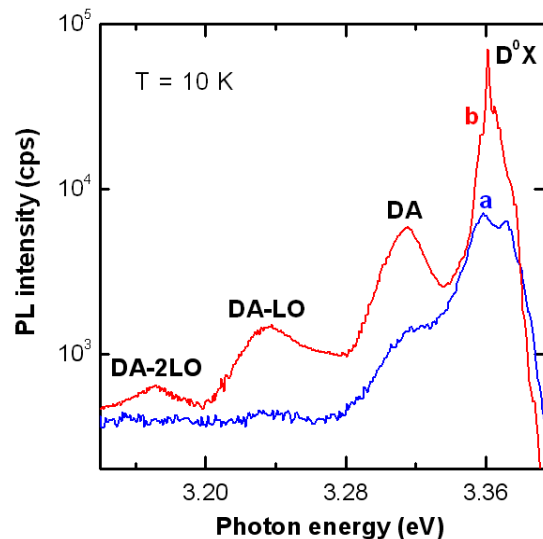


Fig. 4. Near band-edge PL spectra of the samples (a) and (b).

The D^0X bands at 3.61 eV and 3.71 eV correspond to the previously observed I_1 and I_6 bands, the I_6 band being associated with the Al impurity [31]. Apart from the D^0X bands, a PL band is observed at 3.314 eV accompanied by LO phonon replicas, it being previously attributed to the donor-acceptor pair recombination (DA) [32]. At room temperature, the near-band-edge luminescence represents a band due to the recombination of free excitons at 3.30 eV with a LO phonon replica.

As concerns the visible luminescence, taking into account the n-type of the produced material, one can suggest that assignment of these PL bands to the electron transitions from a deep donor level to the valence band ($D-h$ -type recombination) is very improbable [33]. Most probably, these PL bands are due to electronic transitions from the conduction band to acceptor levels ($e-A$ -type recombination). The red band at 1.85 eV is supposed to be associated with a deep unidentified acceptor with the energy level situated close to the middle of the bandgap [34]. The PL bands in the spectral interval of 2.3 – 2.7 eV are most

probably due to different defect complexes involving the V_{Zn} acceptor center. The isolated zinc vacancy is expected to have charge -2 in n -type ZnO where its formation is more favorable. The transition level between the -1 and -2 charge states of V_{Zn} occurs at ~ 0.8 eV above the valence band [34]. Thus, one may expect transitions from the conduction band to the V_{Zn} acceptor at around 2.6 eV in n -type ZnO. Other PL bands observe in this spectral range can be attributed to complex defects involving the V_{Zn} center such as zinc vacancies and zinc antisites ($V_{Zn}-Zn_o$) [35], zinc vacancies and oxygen vacancies [36,37], or more complex defect clusters [38].

The increase of the oxygen content in the Ar/O ratio to 1:1 leads to the emergence of a PL band centered at 2.50 eV instead of bands at 2.37 eV and 2.67 eV which suggest the reconfiguration of the defect complexes (Fig. 3). Apart from that, the near-band-edge luminescence is intensified by an order of magnitude, the D^0X band related to the Al impurity becoming highly predominant (Fig. 4) suggesting an efficient optical activation of this impurity.

Further increase of the oxygen content leads to a spectacular increase of the near-band-edge luminescence intensity by additional several orders of magnitude with a concomitant broadening of the near-band-edge luminescence band. A characteristic feature of this PL band is the broadening toward the Stokes part of the emission. The width of this PL band is 58 meV at 10 K and 115 meV at room temperature. It was previously shown that most probably this PL band is due to direct transitions of electrons from the conduction band tails to valence band tails [39]. The broadening of the PL band involved can be accounted for by the broadening of the band edges due to potential fluctuations induced by the high concentration of intrinsic defects or impurities. This model has been applied to correlate the width of the PL band to the free carrier concentration in highly doped ZnO samples [39]. By using the established dependence, one can estimate that the electron concentration in the sample produced with the Ar:O ratio of 1:10 is $4.0 \times 10^{19} \text{ cm}^{-3}$ at $T = 10 \text{ K}$, and $1.5 \times 10^{20} \text{ cm}^{-3}$ at room temperature. These data suggest that increasing the oxygen content in the Ar/O ratio during the magnetron sputtering promotes the optical and electrical activation of the doping Al impurity.

IV. CONCLUSION

The results of this study demonstrate that the morphology and the luminescence properties of ZnO layers can be controlled by technological parameters of magnetron sputtering. High values of the ratio of argon to oxygen gases in the gas flow during the growth process lead to the production of smooth and flat layers with nearly identical intensity of the near-band-edge and visible luminescence, while the layers obtained with low values of this ratio are porous and exhibit extremely high near-bandgap luminescence intensity.

ACKNOWLEDGMENTS

This work was supported by the Academy of Sciences of Moldova under Contract No. 10.820.05.20/RoF.

REFERENCES

[1] S. Tuzemen, E. Gur, "Principal issues in producing new ultraviolet light emitters based on transparent

- semiconductor zinc oxide", *Opt. Mater.*, vol. 30, pp. 292-310, 2007.
- [2] S. Choopun, H. Tabata, K. Kawai, "Self-assembly ZnO nanorods by pulsed laser deposition under argon atmosphere", *J. Cryst. Growth*, vol. 274, pp. 167-172, 2005.
- [3] M. Huang, S. Mao, H. Feick, H. Yan, Y. Wu, H. Kind, E. Weber, R. Russo, P. Yang, "Room-Temperature Ultraviolet Nanowire Nanolasers", *Science*, vol. 292, pp. 1897-1899, 2001.
- [4] R. Hauschild, H. Kalt, "Guided modes in ZnO nanorods", *Appl. Phys. Lett.* 89, pp. 123107, 2006.
- [5] Y. Y. Naoi, K. Ikeda, T. Hama, K. Ono, R. Choi, T. Fukumoto, K. Nishino, S. Sakai, S. M. Lee, M. Koike, "Blue light emitting diode fabricated on a-plane GaN film over r-sapphire substrate and on a-plane bulk GaN substrate", *Phys. Status Solidi c*, vol. 4, pp. 2810-2813, 2007.
- [6] Z. Zhong, F. Qian, D. Wang, C. M. Lieber, "Synthesis of p-Type Gallium Nitride Nanowires for Electronic and Photonic Nanodevices", *Nano Lett.*, vol. 3, pp. 343-346, 2003.
- [7] F. A. Ponce, D. P. Bour, "Nitride-based semiconductors for blue and green light-emitting devices", *Nature*, vol. 386, pp. 351-359, 1997.
- [8] J. Zhang, L. D. Sun, J. L. Yin, H. L. Su, C. S. Liao, C. H. Yan, "Control of ZnO Morphology via a Simple Solution Route", *Chem. Mater.*, vol. 14, pp. 4172-4177, 2002.
- [9] B. Liu B. H. C. Zeng, "Hydrothermal Synthesis of ZnO Nanorods in the Diameter Regime of 50 nm", *J. Am. Chem. Soc.*, vol. 125, pp. 4430-4431, 2003.
- [10] H. L. Cao, X. F. Qian, Q. Gong, W. M. Du, X. D. Ma, Z. K. Zhu, "Shape- and size-controlled synthesis of nanometre ZnO from a simple solution route at room temperature", *Nanotechnology*, vol. 17, pp. 3632-2636, 2006.
- [11] S. T. Shishiyanu, O. I. Lupan, E. V. Monaico, V. V. Ursaki, T. S. Shishiyanu, I. M. Tiginyanu, "Photoluminescence of chemical bath deposited ZnO:Al films treated by rapid thermal annealing", *Thin Solid Films*, vol. 488, pp. 15-19, 2005.
- [12] V.V. Ursaki, O.I. Lupan, L. Chow, I.M. Tiginyanu, V.V. Zalamai, "Rapid thermal annealing induced change of the mechanism of multiphonon resonant Raman scattering from ZnO nanorods", *Solid State Communications*, vol. 143, pp. 437-441, 2007.
- [13] G. Westin, A. Ekstrand, M. Nygren, R. Österlund, P. Merkelbach, "Preparation of ZnO-based varistors by the sol-gel technique", *J. Mater. Chem.*, vol. 4, pp. 615-621, 1994.
- [14] S.-Y. Chu, T.-M. Yan, S.-L. Chen, "Characteristics of sol-gel synthesis of ZnO-based powders", *J. Mater. Sci. Lett.*, vol. 19, pp. 349-352, 2000.
- [15] W. I. Park, D. H. Kim, S. W. Jung, G. C. Yi, "Metalorganic vapor-phase epitaxial growth of vertically well-aligned ZnO nanorods", *Appl. Phys. Lett.*, vol. 80, pp. 4232-4235, 2002.
- [16] Y. J. Zeng, Z. Z. Ye, W. Z. Xu, L. P. Zhu, B. H. Zhao, "Well-aligned ZnO nanowires grown on Si substrate via metal-organic chemical vapor deposition", *Appl. Surf. Sci.*, vol. 250, pp. 280-283, 2005.

- [17] A. Burlacu, V. V. Ursaki, V. A. Skuratov, D. Lincot, T. Pauporte, E. V. Rusu, I. M. Tiginyanu, "The impact of morphology upon the radiation hardness of ZnO layers", *Nanotechnology*, vol. 19, 215714, 2008.
- [18] El-Shaer, A. Che Mofor, A. Bakin, M. Kreye, A. Waag, "High-quality ZnO layers grown by MBE on sapphire", *Superlattices and Microstructures*, pp. 265-271, 2005.
- [19] H. Kato, M. Sano, K. Miyamoto, T. Yao, B.-P. Zhang, K. Wakatsuki, Y. Segawa, "MBE growth of Zn-polar ZnO on MOCVD-ZnO templates", *Phys. Status Solidi (b)*, vol. 241, pp. 2825-2829, 2004.
- [20] T. Pauporté, D. Lincot, "Heteroepitaxial electrodeposition of zinc oxide films on gallium nitride", *Appl. Phys. Lett.*, vol. 75, pp. 3817-3820, 1999.
- [21] M. J. Zheng, L. D. Zhang, G. H. Li, W. Z. Shen, "Fabrication and optical properties of large-scale uniform zinc oxide nanowire arrays by one-step electrochemical deposition technique", *Chem. Phys. Lett.*, vol. 363, pp. 123-128, 2002.
- [22] O. Lupan, T. Pauporte, B. Viana, I. M. Tiginyanu, V. V. Ursaki, and R. Cortes, *Epitaxial Electrodeposition of ZnO Nanowire Arrays on p-GaN for Efficient UV-Light-Emitting Diode Fabrication*, *ACS J. Appl. Materilas and Interfaces*, 2, No. 7, 2083-2090 (2010).
- [23] S. Y. Li, C. Y. Lee, T. Y. Tseng, "Copper-catalyzed ZnO nanowires on silicon (1 0 0) grown by vapor-liquid-solid process", *J. Cryst. Growth.*, vol. 247, pp. 357-362, 2003.
- [24] P. X. Gao, Z. L. Wang, "Nanoarchitectures of semiconducting and piezoelectric zinc oxide", *J. Appl. Phys.* 97, 044304, 2005.
- [25] F. Xu, K. Yu, G. Li, Q. Li, Z. Zhu, "Synthesis and field emission of four kinds of ZnO nanostructures: nanosleeve-fishes, radial nanowire arrays, nanocombs and nanoflowers", *Nanotechnology*, vol. 17, 2855-2859, 2006.
- [26] C. Li, G. Fang, F. Su, G. Li, X. Wu, X. Zhao, "Synthesis and photoluminescence properties of vertically aligned ZnO nanorod-nanowall junction arrays on a ZnO-coated silicon substrate", *Nanotechnology*, vol. 17, 3740-3744, 2006.
- [27] Y. H. Yang, B. Wang, G. W. Yang, "Growth mechanisms of one-dimensional zinc oxide hierarchical structures", *Nanotechnology*, vol. 17, 5556-5560, 2006.
- [28] V. V. Ursaki, E. V. Rusu, A. Sarua, M. Kuball, G. I. Stratan, A. Burlacu, I. M. Tiginyanu, "Optical characterization of hierachical ZnO structures grown with a simplified vapour transport method", *Nanotechnology*, vol. 18, 215705 (2007).
- [30] K. Vanheusden, C. H. Seager, W. L. Warren, D. R. Tallant, J. A. Voigt, "Correlation between photoluminescence and oxygen vacancies in ZnO phosphors", *Appl. Phys. Lett.*, vol. 68, pp. 403-405, 1996.
- [31] R. M. Nyffenegger, B. Craft, M. Shaaban, S. Gorer, G. Erley, R. M. Penner, "A Hybrid Electrochemical/Chemical Synthesis of Zinc Oxide Nanoparticles and Optically Intrinsic Thin Films", *Chem. Mater.*, vol. 10, pp. 1120-1129, 1998.
- [32] Meyer B K et al., "Bound exciton and donor-acceptor pair recombinations in ZnO", *Phys. Stat. Sol. (b)*, vol. 241, pp. 231-260, 2004.
- [33] V.V. Ursaki, I.M. Tiginyanu, V.V. Zalamai, V.M. Masalov, E.N. Samarov, G.A. Emelcenko, F. Briones, "Photoluminescence of ZnO layers grown on opals by chemical deposition from zinc nitrate solution", *Semiconductor Science and Technology*, vol. 19, pp. 851-854, 2004.
- [34] M. A. Reshchikov, R. Y. Korotkov, "Analysis of the temperature and excitation intensity dependencies of photoluminescence in undoped GaN films", *Phys. Rev. B*, vol. 64, 115205, 2001.
- [35] U. Ozgur, Ya. I. Alivov, C. Liu, A. Teke, M. A. Reshchikov, S. Doğan, V. Avrutin, S.-J. Cho, H. Morkoç, "A comprehensive review of ZnO materials and devices", *J. Appl. Phys.*, vol. 98, 041301, 2005.
- [36] Z. Q. Chen, K. Betsuyaku, A. Kawasuso, "Vacancy defects in electron-irradiated ZnO studied by Doppler broadening of annihilation radiation", *Phys. Rev.*, vol. B 77, 113204, 2008.
- [37] S. A. Studenikin, M. Cocivera, "Time-resolved luminescence and photoconductivity of polycrystalline ZnO films", *J. Appl. Phys.*, vol. 91, pp. 5060-5064, 2002.
- [38] J. Zhong, A. H. Kitai, P. Mascher, W. Puff, "The influence of processing conditions on point defects and luminescence centers in ZnO", *J. Electrochem. Soc.*, vol. 140, pp. 3644-3649, 1993.
- [39] Y. Dong, F. Tuomisto, B. G. Svensson, A. Yu. Kuznetsov, L. J. Brillson, "Vacancy defect and defect cluster energetics in ion-implanted ZnO", *Phys. Rev. B*, vol. 81, 081201(R), 2010.
- [40] V.V. Zalamai, V.V. Ursaki, E. Rusu, P. Arabadji, I.M. Tiginyanu, L. Sirbu, "Photoluminescence and resonant Raman scattering in highly conductive ZnO layers", *Appl. Phys. Lett.*, vol. 84, pp. 5168-5170, 2004.